X-615-69-500
PREPRINT

NASA TM X-65548

A NEAR INFRA-RED RADIOMETER FOR USE ON SMALL SOUNDING ROCKETS

JEAN WELKER
W. H. JONES

NOVEMBER 1969

GSFC — GODDARD SPACE FLIGHT CENTER —
GREENBELT, MARYLAND

X-615-69-500

A NEAR INFRA-RED RADIOMETER FOR USE ON SMALL SOUNDING ROCKETS

Jean Welker
W. H. Jones

November 1969

GODDARD SPACE FLIGHT CENTER
Greenbelt, Maryland

A NEAR INFRA-RED RADIOMETER FOR USE ON SMALL SOUNDING ROCKETS

Jean Welker and W. H. Jones
Laboratory for Space Sciences
Goddard Space Flight Center
Greenbelt, Maryland

ABSTRACT

An infra-red radiometer was designed, developed and calibrated in the Ionospheric and Radio Physics Branch of the Space Sciences Division within a period of two months in September - October 1968. The radiometer was subsequently flown on a Nike Apache flight from Wallops Island, Va. on November 19, 1968.

The radiometer was designed to measure the radiation emission from the molecular transition O_2 ($a^1\Delta_g$ - $X^3\Sigma_g^-$) which is centered at 1.268μ. This radiometer looked out the side of the rocket, that is to say, in a direction perpendicular to the cylindrical axis of the rocket. Usually, radiometers of this type are mounted so that they view a direction through the nose along the cylindrical axis of the rocket. The advantages and disadvantages of such a mounting configuration are discussed as well as complete design considerations and the calibration procedures.

CONTENTS

A NEAR INFRA-RED RADIOMETER FOR USE ON SMALL SOUNDING ROCKETS

1. INTRODUCTION

Multi-experiment payloads have been built and flown over the last few years on Nike-Apache rockets to obtain data on the D-region of the Ionosphere during the daytime. In order to discover the role played by excited oxygen molecules in the D region chemistry, a radiometer was designed to fly on these payloads and detect the emission produced by the transition O_2 ($a^1\Delta_g - X^3\Sigma_g^-$). This emission transition is a band over 200 Å wide which is centered at 1.268μ. The radiometer had to be small in size and weight and inexpensive to build since the packages are not recovered. It had to distinguish this emission level from the background during the day and therefore had to have a channel to monitor the background in addition to the signal channel. One of these instruments has been flown from Wallops Island, Va.

The restrictions were numerous. The radiometer had to be light in weight (two to three pounds) and small in size (less than six inches in height with the six inch rocket shelf diameter). The radiometer also was required to have the sensitivity to detect the signal level above the background (maximum estimated signal level was 10^7 Rayleighs) and the response time necessary to resolve the signal while looking out the side of a rapidly spinning rocket (rocket spin is usually from 5 to 10 cps). Also, the radiometer was required to detect signal levels in two spectral regions, the 1.268μ region which corresponds to the transition for O_2 ($a^1\Delta_g - X^3\Sigma_g^-$) and the nearby 1.23$\mu$ region which was used as a background region. Both the 1.268μ and the 1.23μ wavelength designations represent the center wavelengths

of 100 Å wide transmission bands of the filters. The radiometer alternately looks at the signal plus background region of the 1.268μ pass band and the background region of the 1.23μ pass band, subtracting the background from the signal plus background.

2. DESCRIPTION

Filters

The filters used were obtained from Infra-Red Industries, Thin Film Division, Waltham, Mass. The filters were centered on the wavelengths 1.23μ and 1.268μ. Plots of the transmission curves are shown in Figures 1 and 2, and were obtained with a Cary 14 spectrophotometer. The transmission of the filters outside the passband was less than 1%. The integrated transmission over the entire transmission range was in the neighborhood of 50% as can be seen from Figures 1 and 2.

Lens

The radiometer used a single lens of diameter 14.5 mm and of focal length 25 mm. The transmittance of the lens was estimated to be of the order of 90% in the wavelength region used. The PbS detector was placed at the focal point of the lens.

Detectors

PbS detectors were used in the radiometer and these detectors were obtained from the Santa Barbara Research Corporation, subsidiary of Hughes Aircraft Corporation. The light sensitive area of these detectors was 4 mm × 4 mm. The light sensitive area on one of the two detectors used was blackened and this

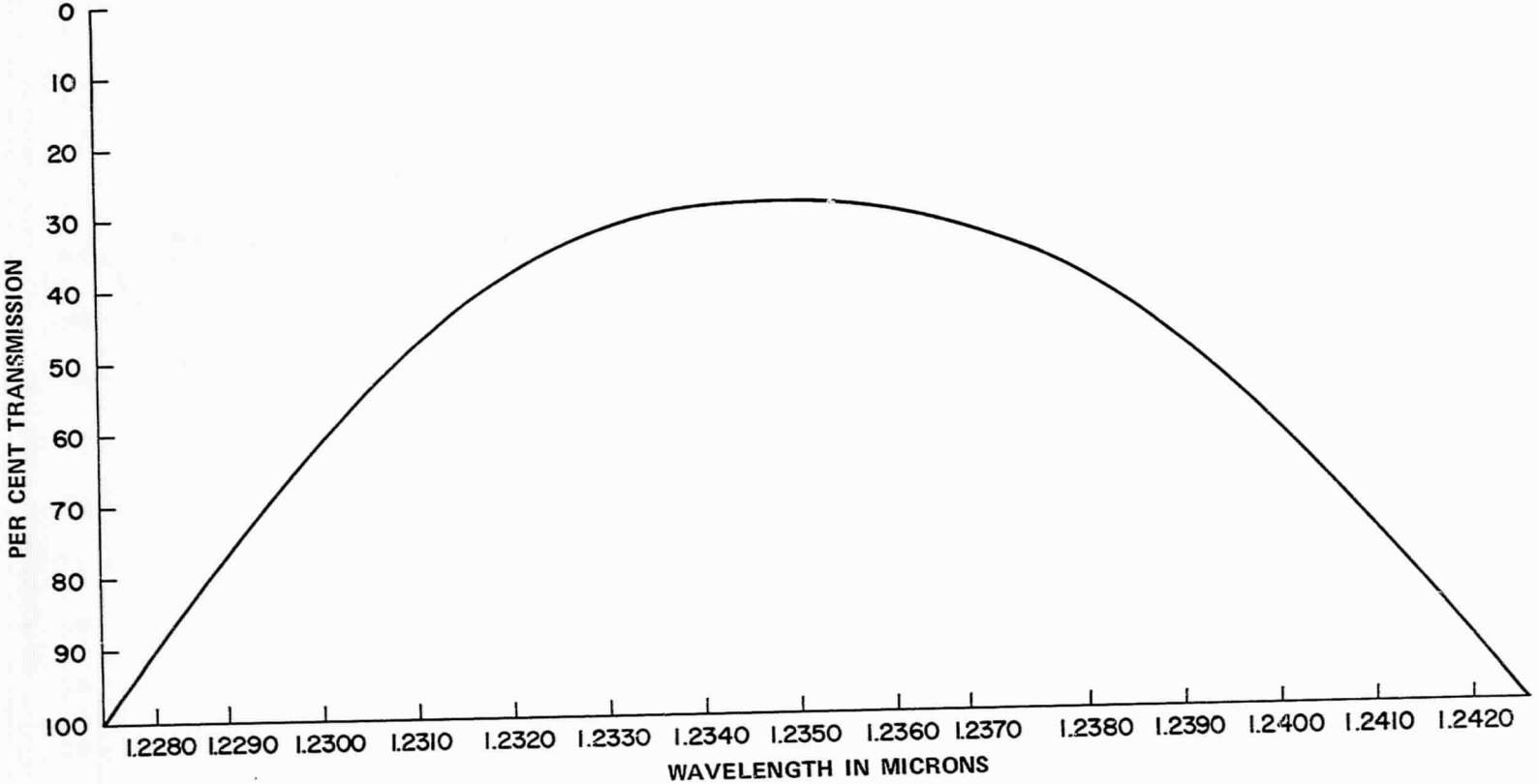

Figure 1. 1.234 μ Filter Transmission Curve

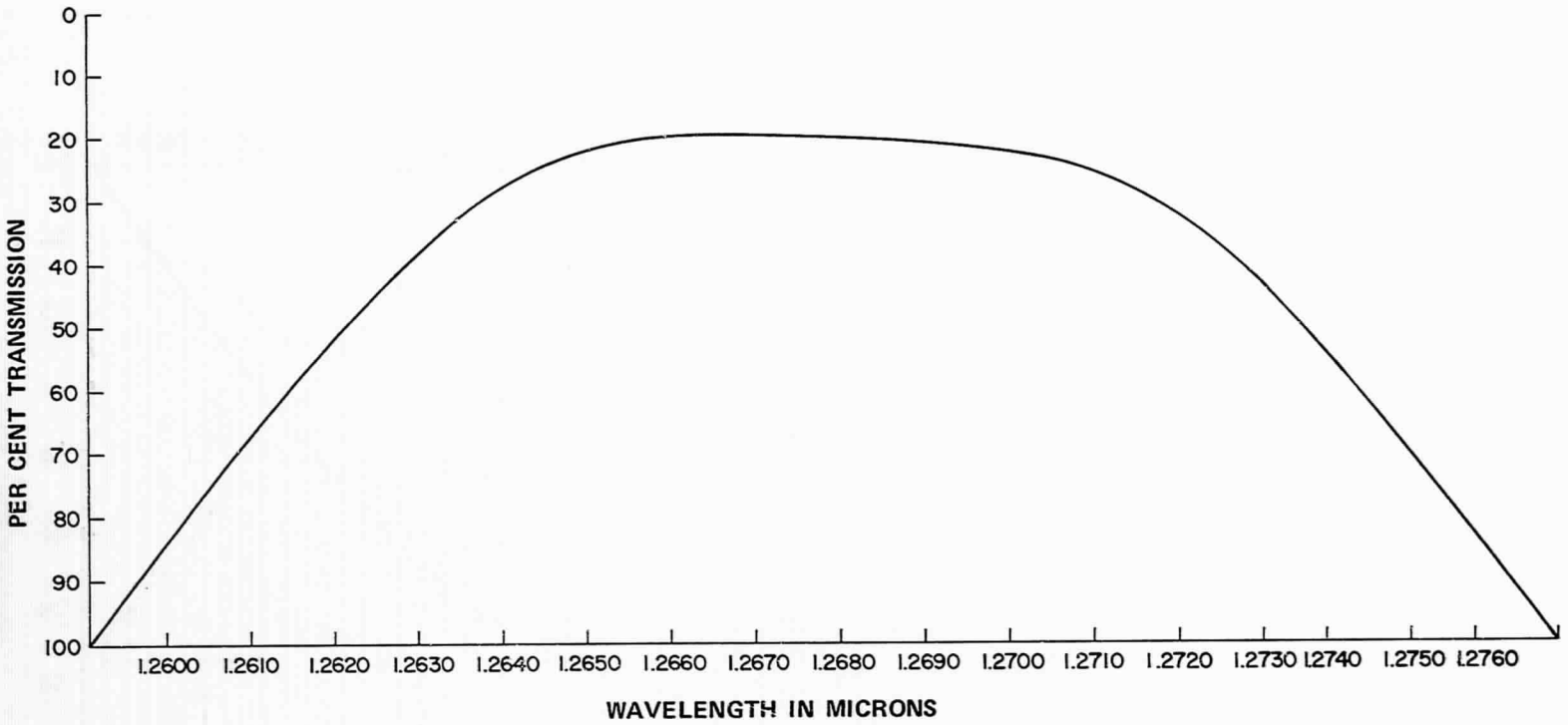

Figure 2. 1.268μ Filter Transmission Curve

blackened detector was then used as a complementary load resistor in the simple bridge configuration shown in Figure 3. Equal bias voltages of opposite polarity were applied across the detectors, keeping their common junction close to ground potential to minimize noise due to leakage currents and microphonics. Since the characteristics of the two detectors were matched, both tended to exhibit similar resistance changes when ambient temperature changes occurred. Consequently, the potential of their common junction remained essentially at zero. Since the active detector's internal impedance was equal to the impedance of the compensating blackened detector, maximum power transfer was obtained over a temperature range. The photon efficiency of PbS increases with decreasing temperature. At ambient temperatures, the photon efficiency decreases by approximately 4% per degree centigrade. The resultant temperature effect was to change the detector output for a constant input flux. The light sensitive detector and the blackened load resistance detector were physically mounted touching back to back in the radiometer in order to more nearly maintain the same temperature on both components. Characteristics of both detectors are listed below:

Test Conditions

Blackbody Temperature:	500°K
Blackbody Flux Density:	6.54×10^{-6} watts/cm^2
Chopping Frequency:	789 Hz
Noise Bandwidth:	80 Hz
Bias Voltage:	100 volts
Load Resistance:	0.50 megohm
Detector Temperature:	295.8°K

The light sensitive detector had R_c = 0.45 megohms

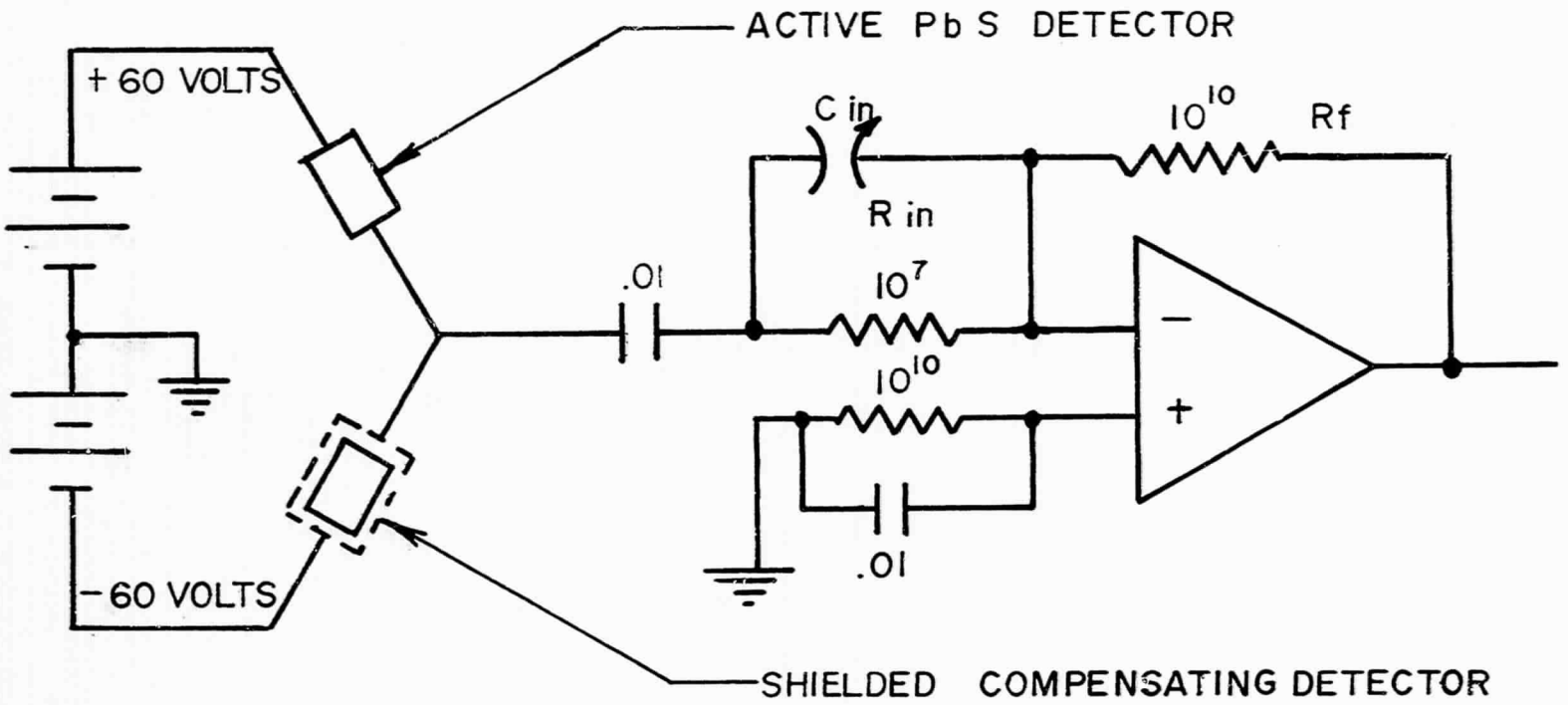

Figure 3. Detector Configuration

Test Conditions

Noise (RMS):	1.8 volts
Signal:	420 millivolts
D* (500°K, 780 Hz):	8.0×10^8 cm $Hz^{1/2}$/watt
Calculated D* (6,780 Hz):	8.4×10^{10} cm $Hz^{1/2}$/watt

The blackened load resistance had a dark resistance R_c = 0.47 megohms.

3. PERFORMANCE

The design considerations were dictated by the characteristics of the flight. The radiometer was to be flown on a Nike-Apache rocket which was to rise at the rate of a kilometer a second with a spin rate of 5 to 10 revolutions per second, or, at the faster rate, one spin every 200 milliseconds. The integrating time on the integrator circuit was set at 50 milliseconds which was one fourth or 90° of every 360° of rocket spin. Since the filter wheel was set to rotate at the rate of 120 cps or one revolution every 8 milliseconds, the integrator circuit was storing six rotations of the filter wheel. The response time of the detector was in the range of 0.5 to 1.0 millisecond and therefore, produced no limiting effect on the response time of the radiometer. Response times of the electronics were much faster than those of the detector and also had no limiting effect on the operation.

The signal to noise ratio of the detector was not used to advantage since the noise in the electronic circuitry was greater than the noise in the detector and the motor, which was used to rotate the filter, had even a greater noise level than the electronic circuitry. An estimate of the motor noise level was 50 millivolts but with temperature fluctuations and all other variations, a more conservative extimate would place the noise level at 100 millivolts. This noise level resulted

in a maximum dynamic operating range of 40 to 1, since the telemetering response was from 1 to 5 volts positive or over a full 4 volt dynamic range for the 1.268μ signal region level greater than the 1.23μ background region level. Consideration was taken of the situation in which the 1.23μ radiation level is greater than the 1.268μ level. The radiometer was set for a 1 volt positive offset zero level to allow it to record as much as 1 volt deflection in the negative direction from the zero setting. This deflection in the negative direction below the zero level setting will occur when the 1.23μ radiation level is greater than the 1.268μ level.

This situation can occur, for example, when the temperature is so high that the 1.23 and 1.268μ, 100 Å pass bands are both shifted past the peak to the backside and negative slope of a black body curve; in this case the 1.23μ radiation level is always greater than the 1.268μ radiation level if we disregard any drastic attenuation conditions which may exist.

As for the actual level of radiation in the 1.268μ pass band that gets through to the detector, an estimate can be made by considering the maximum level of signal radiation expected in flight (in this case approximately 10 Megarayleighs) and then converting this amount through the various attenuating restraints of the radiometer. The radiant flux incident on a detector from an extended airglow source is given by

$$P = N A \Omega$$

where

P - radiant flux in watts
N - radiance in watts/cm^2/stear
A - area of the lens aperature in cm^2
Ω - field of view of the detector in stearadians

If a lens aperature of 1.45 cm diameter is chosen, the lens area is

$$A = \frac{\pi D^2}{4} = 1.65 \text{ cm}^2$$

With a planer field of view angle of $\theta = 2.1°$ (half cone angle)

$$\Omega = 2\pi (1 - \cos \theta)$$

$$\Omega = 2\pi (1 - \cos 2.1°) = 1.34\pi \times 10^{-3}$$

As previously stated, the maximum radiant intensity of the signal is estimated to be 10^7 Rayleighs for the 1.268μ emission band. (1 Rayleigh = 10^6 photons/ cm^2/sec)

Since

$$N = \frac{1}{4\pi} R = \frac{1}{4\pi} 10^6 \times 10^7 = \frac{1}{4\pi} \times 10^{13} \text{ photons/cm}^2\text{/sec/stear}$$

where R - photon flux (photons/cm^2/sec) and at 1.268μ, 1 watt = 6.39×10^{18} photons/sec. Then

$$N = \frac{1}{4\pi} \times 10^{13} \times \frac{1}{6.39} \times 10^{-18} = \frac{1.565}{4\pi} \times 10^{-6} \text{ watts/cm}^2\text{/stear}$$

The radiant flux incident on the detector can now be considered.

$$P = N A\Omega = \frac{1}{4\pi} \times 8.89 \times 10^{-10} \text{ watts}$$

To this figure, consideration must be taken of the losses due to reflection and absorption of the lens and filters. As previously mentioned, there is a 10% absorption

in the lens and a 50% absorption over the bandpass in the filters. The effective transmission is then only 40% and therefore, the power incident on the detector is

$$P = .40 \times 8.89 \times 10^{-10} = 3.56 \times 10^{-10} \text{ watts.}$$

4. ELECTRONICS

General Discussion

The method used to detect the infra-red radiation and to amplify the subsequent voltage level change obtained to a usable level is shown in Figure 4. This method has been used for many years in laboratory work (Ref. 1) and now has been adopted for sounding rocket use. The incoming infra-red radiation is chopped by a rotating wheel rim on which two semi-circular interference filters are mounted. The radiation falling on the detector, therefore, passes alternately through the two filters. This produces a signal appearing at the input of the amplifier which has an amplitude proportional to the difference in flux passing through the two filters and a frequency dependence determined by the chopping rate of the filter wheel. The resulting signal produced is then amplified, demodulated and sent to the telemeter.

Detector Bias

The bias for the detection bridge shown in Figure 3 is supplied by a stack of Leclanché cells. These batteries exhibit a temperature coefficient of 0.003% per degree centigrade, (Ref. 2). For small changes in the bias voltage, the detector responds in a linear fashion and consequently, the effect of bias variation is small compared to the effect of temperature on the detector. The battery supply

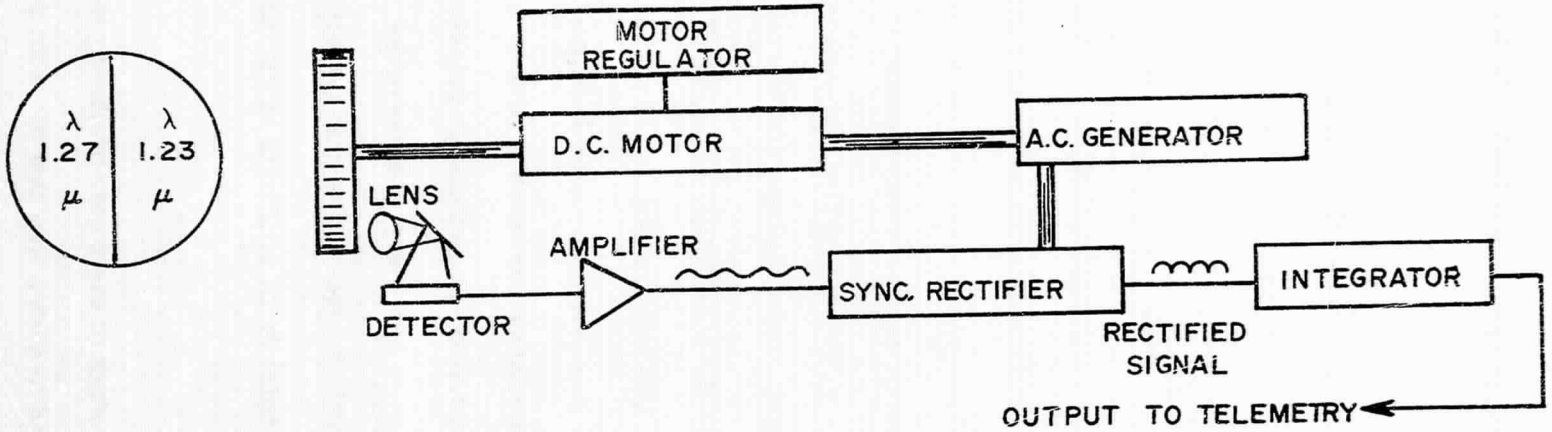

Figure 4. Radiometer Schematic

consisted of eight 15 volt batteries, (Burgess, Batteries Model Y-10) and were connected 48 hours before the rocket launch to allow the batteries to stabilize.

Amplifier

A commercially available operational amplifier (Zeltex Inc. Model 162) is used to amplify the detector signal. The amplifier achieves high input impedance and low bias current through the use of a field effect transistor input stage. The amplifier is mounted on a ceramic substrate which produces good thermal tracking and the unit is then solid potted to reduce microphonics. The amplifier has an open loop gain greater than 2×10^5 and the gain bandwidth produce is 4 megahertz. From Figure 3, the closed loop gain of the amplifier is 10^3, simply the ratio of R_f to R_{in}. The input time constant ($R_{in}C_{in}$) was adjusted to equal the feedback time constant (R_f C_{stray}) in order to maintain a flat response from 40 Hertz to 4×10^3 Hertz. The high frequency response is needed even with the filter wheel chopping rate of 120 cps, since the wave shape is traposoidal thus necessitating a high band pass amplifier. The input impedance of the circuit is R_{in} which is 10^7 megohms. However, the detector impedance drift produces a resulting change in gain for the detector amplifier combination of only 0.1% per degree centigrade since R_{in} is initially 20 times larger than the impedance of the detector. The amplifier temperature drift is further reduced by the value of R_2, resulting in an overall temperature drift of a few millivolts per degree centigrade at its output. Amplifier electronic noise is 20 millivolts at the output.

Synchronous Rectifier

An A.C. generator is attached to the rear shaft of the motor producing the filter wheel chopping and the generator is phased in such a way that the A.C. waveform

passes through zero when the optical filter passes from one wavelength to another. This A.C. waveform is then fed into a squaring circuit which then generates a waveform suitable for driving a flip flow switching circuit. Two outputs are taken from the flip flop circuit, each output 180° out of phase with the other. These outputs are then used to operate a pair of MOS-FET switches. The opening and closing of these switches then has a fixed relationship to the two filters on the rotating filter wheel.

At this point, the analog signal is taken from the output of the amplifier as shown in Figure 5, and fed into a second amplifier with an overall gain of unity. This second amplifier has two outputs, one which is inverted, the other which is not. The net effect of this second amplifier is the production of a fully rectified signal level from the two filters on the filter wheel. When this rectifier amplifier is tied to the two MOS-FET switches previously discussed, the resultant combination is a synchronous rectifier circuit which has the ability to distinguish and separate the signal levels from each of the two filters. The output signal of this synchronous rectifier circuit, when filtered to remove the 120 Hertz carrier, is then proportional to the difference in the flux through the two optical filters. The final amplifier in Figure 5 has a gain of five and is used to isolate the switches and to act as a line driver. The type of detection system just described has a much higher signal to noise ratio than a non-coherent signal detection system since it can eliminate noise which does not remain in phase with the signal. For example, low frequency noise such as 1/f noise is eliminated while on the high frequency end, noise components such as flicker and shot noise are also removed.

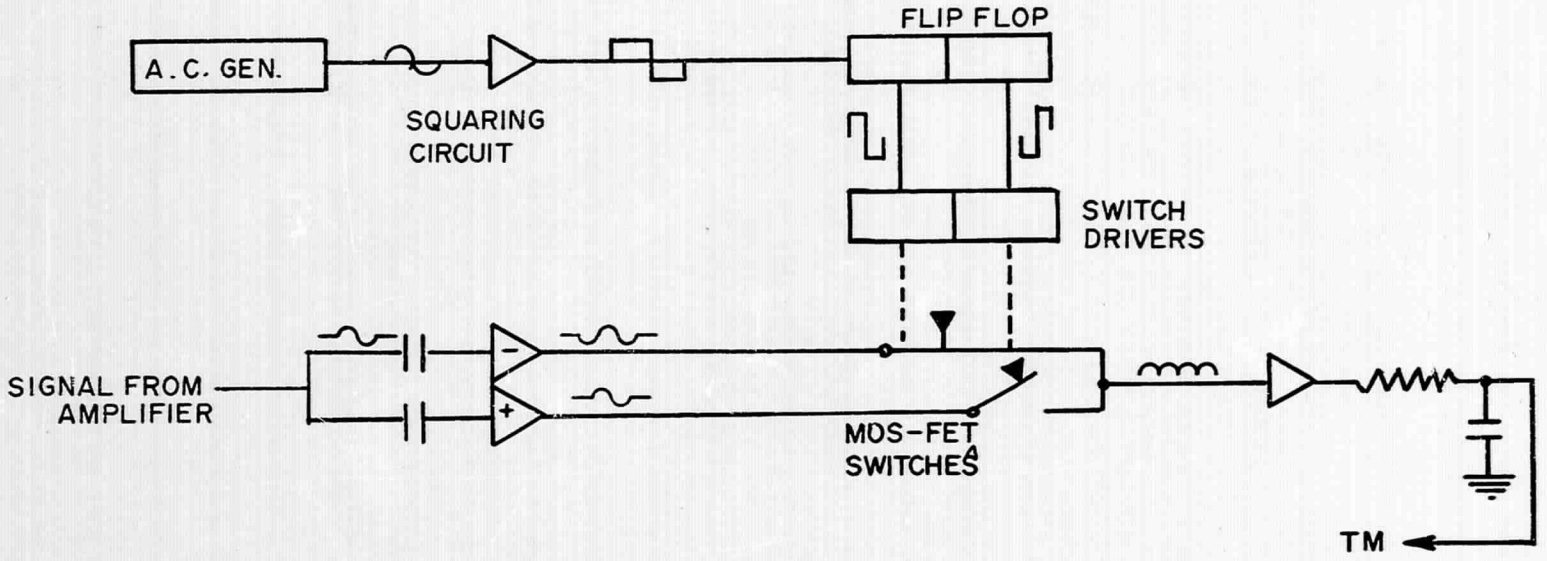

Figure 5. Synchronous Amplification Schematic

In the discussion of the synchronous generator, it was mentioned that MOS-FET switches were used. MOS-FET switches were chosen rather than bipolar switches for a few reasons. When the MOS-FET switches are conducting, they lack semiconductor junctions in the signal path and their subsequent temperature dependence. The resistance of these devices in the conducting mode is a few hundred ohms, and variations due to temperature and sample to sample differences are overpowered by the high impedance of the final amplifier. The non-conduction mode resistance is in excess of 10^4 megohms and for this application, this resistance constitutes and open circuit. Because of the high degree of isolation of insulated gate transistors, there are no error voltages introduced by coupling from the synchronous drive circuits to the data channel.

Motor and Motor Regulator

The motor which is used to turn the chopping filter wheel is a miniature dual shafted device with dry bearings to allow for operation for extended periods in vacuum. It was not necessary to regulate the motor speed since there are no tuned or frequency dependent circuits with the exception of the output integrator. This integrator circuit is solely responsible for the determination of the data bandpass. The motor speed was found to increase by 30% when the ambient pressure was reduced from atmospheric to vacuum. Since the response time of the amplifiers and the detector is much faster than the 30% variation in chopping speed, this variation effectively does not change the gain. Since the change in gain was not a factor, the purpose of the motor regulator circuit was to isolate and suppress motor transients. This was accomplished with shielding and an array of filters. The main source of noise within the radiometer system was

microphonics due to vibration caused by the 120 cps rotation of the filter wheel. These microphonics were drastically reduced by careful balancing of the rotational parts. The stages of improvement in the reduction of vibration were carefully measured with sensitive vibration monitoring equipment as well as the monitoring of the electronic noise due to the microphonics. With as much care as possible, the level of noise could not be reduced below a level equivalent to an input radiation at 1.27μ of 0.3 Megarayleighs. This can be compared to a maximum expected signal level in the airglow of 10 to 20 Megarayleighs.

5. CALIBRATION

The distribution of radiation varies with respect to wavelength, spatial position, direction, time or frequency and polarization. In addition to the variation of the radiation intensity from the source with respect to these parameters, the radiometer itself characteristically distorts each of these parameters in its own way. Further, there are environmental and instrumental changes which also affect the responsivity of the detector, a prime example of which is the change in the detector element temperature. All these factors and their effect on the linearity, gain and overall reliability of the instrument should be determined to the highest degree of accuracy attainable.

Initially the only calibration source available to this project with sufficient power and of an extended source variety was an integrating sphere located at Goddard Space Flight Center in Greenbelt, Maryland. The sphere has the physical dimensions of a six foot diameter with an exit aperature diameter in the skin of the sphere of four inches and was coated white inside to provide a high reflectivity. The active radiation source consists of twelve lamps located inside the sphere

around the exit aperature. A calibration had been made of the sphere and a comparison with a black body spectral distribution for both voltage settings and number of lamps had been calculated. Table 1 shows the reduction in intensity with number of lamps. Table 2 shows the integrating sphere's comparative black body spectrum. Radiation levels produced by the sphere were too high for the radiometer and a series of neutral density filters were used to bring the radiation levels down to usable magnitudes. For a further discussion of the calibration sphere see Reference 3.

Table 1

Ratio of Intensity of N Lamps To 12 Lamps In Spherical Integrator

Number of Lamps	$W_{\lambda n}/W_{\lambda 12}$
12	1.0000
11	.9154
10	.8310
9	.7468
8	.6627
7	.5782
6	.4962
5	.4115
4	.3286
3	.2471
2	.1640
1	.08215

Table 2

Spectral Radiant Emittance of Six-Foot Spherical Integrator

(λ in microns; W_λ in milliwatts $\cdot$ cm^{-2} $\cdot$ μ^{-1})

λ	W_λ	λ	W_λ
		1.1	170
.32	.136	1.2	132
.35	.745	1.3	106
.37	1.99	1.4	48.0
.40	6.24	1.5	40.7
.45	20.3	1.6	36.5
.50	47.3	1.7	20.6
.55	84.8	1.8	13.1
.60	139	1.9	6.82
.65	176	2.0	5.32
.70	204	2.1	4.77
.75	237	2.2	3.92
.80	263	2.3	1.73
.90	249	2.4	1.05
1.00	209	2.5	.665
		2.6	.252
		2.7	.140

The integrating sphere provided only variation in magnitude of radiation for and extended field of view source. With the purchase of a Barnes Engineering Company collimator and black body we were able to obtain a calibration with the accuracy and diversity necessary for a radiometer of this type. The black body used was the Barnes Corporation Blackbody Simulator 11-200T in conjunction with a 6-101 Off-Axis Collimator. The Collimator's reflecting optics had a special coating of iron-seeded gold and silicon monoxide which prevented the usual dip in the reflectance curve at 0.8μ which is so characteristic of other coatings. With this coating, the reflectance curve for the entire collimator is essentially flat over the spectral range from 0.7 to 2.0μ and the reflectance is about 78%. A 11-200/201-10 Modulator Unit was also added to the off-axis collimator which allowed the source signal to be chopped at variable speeds. The black body has a maximum temperature setting of 1000°C. This temperature setting produces an irradiance, E, of 6×10^{-8} watts/cm^2 for the 100 Å pass band centered on 1.268μ and an irradiance of 5×10^{-8} watts/cm^2 for the 100 Å pass band centered on 1.23μ. Since the radiometer reads the difference between the two irradiance levels, the net signal irradiance for detection is 1.0×10^{-8} watts/cm^2 to the front face of the filter without considering the area of the optical system, the solid angle of the field of view, or the attenuation of the filters and optics.

The linearity of response (constant of responsivity a function of input level) was the first calibration measurement that was made. This measurement was made with both the integrating sphere and the black-body collimator sources. For the sphere, the intensity of radiation was varied with the use of neutral density filters and number of lamps used. The intensity of collimated black-body source was

varied by changing the collimator entrance aperature size as well as changing the temperature of the black-body.

For the special responsitivity calibration, that is, the determination of the change in responsivity with respect to position and direction, the collimated black body in the near extended source configuration was used. Usually, one of the first things that is done in the mapping of the field of view. An exception can be made to this rule when the radiometer is required only to measure the radiance of uniformity emitting extended sources, the assumption being that there is no doubt that the entire field of view is always filled. For our particular case, we fulfill most of the requirements for an extended uniformly illuminated field of view, at least in the region where we expect to see the data. The exception to this rule occurs when a strong signal from the sun enters the field of view of the radiometer. At this point, in terms of gathering a signal from the emission of O_2 molecules distributed in the sky, the data collection period is over until the sun disappears from the radiometer's field of view. However, the angular distance at which the sun can first make its appearance is of prime importance in the determination of the signal recording region. Therefore, an extremely strong signal was used to test the angular field of view in all directions. Finally, the radiometer's responsivity as a function of angle of incidence on the entrance pupil of the radiometer was determined with the collimated black-body. The calibration procedure requires that the angle, θ, which is the angle between the optical axis of the radiometer and the collimator, be varied in such a way that the intersection of these two axis is always taken at the center of the radiometer entrance pupil. When this procedure is followed, the aperature of the radiometer is always completely illuminated although it is obvious from the figure, that the exit pupil of

the collimator must be somewhat larger than the entrance pupil of the radiometer.

The most critical calibration for our particular application is the temporal (frequency) responsivity calibration. It was desirable in this case to establish a temporal responsivity calibration in two ways. As previously discussed, the radiometer looked out the side of the rocket which was spinning at a rate of 5 cps around its cylindrical axis. The radiometer, therefore, turned through an angle of 360° every 200 milliseconds. During 50 milliseconds or 90° of this rotation, the radiometer was reacting violently due to the fact that it had looked in the direction of the sun. For the other 150 milliseconds of the rotation, it appeared to have recovered and was producing realistic signal levels. The data was taken at that point in the spin rotation where the sun's radiation was least likely to affect the performance of the radiometer. Therefore, the recovery time of the radiometer from a strong source equivalent to an indirect look at the sun had to be established, as well as the normal change in responsivity at the expected O_2 emission intensity levels with signal shopping frequency. This second calibration of responsivity with frequency is that which would be normally considered the frequency responsivity calibration for a radiometer of this type.

REFERENCES

1. The Detection and Measurement of Infra-Red Radiation, Smith, R. A., Jones, F. E. and Chasmar, R. P., Oxford University Press, London, (1957).

2. Electrical Characteristics of Day Cells and Batteries, U. S. Bureau of Commerce, National Bureau of Standards, LC 965, 1949.

3. Evaluation and Calibration of Some Energy Sources for the Visible and Near Infra-Red Regions of the Electromagnetic Spectrum, McCulloch, A. W., McLean, J. T., Mohr, E. I., NASA GSFC, X-622-69-195, May, 1969.